ISSN 0915-633X

NATIONAL INSTITUTE FOR FUSION SCIENCE

Charge Inversion of a Spherical/Rod Macroion under Different Coion and Monovalent Salt Conditions: Electrophoresis by Molecular Dynamics Simulations

M. Tanaka and A.Yu. Grosberg

(Received - Sep. 20, 2002)

NIFS-755 Oct. 2002

RESEARCH REPORT
NIFS Series

TOKI, JAPAN

Charge Inversion of a Spherical/Rod Macroion under Different Coion and Monovalent Salt Conditions: Electrophoresis by Molecular Dynamics Simulations

Motohiko Tanaka
National Institute for Fusion Science, Toki 509-5292, Japan

A.Yu.Grosberg
Department of Physics, University of Minnesota, Minneapolis, MN 55455

By molecular dynamics simulations we study the effects of coion radius and valence and those of monovalent salt on the electrophoretic mobility of a charge-inverted spherical or rod macroion. For the parameter windows examined, the reversed mobility increases with the ratio of coion to counterion radii a^-/a^+, which peaks at $a^-/a^+ \approx 1.5$. It decreases with the ratio of coion to counterion valences Z^-/Z^+, and becomes non-reversed for $Z^-/Z^+ > 1$. The monovalent salt suppresses reversed mobility when its ionic strength exceeds that of the adsorbed counterions, except for mobility enhancement of a strongly charged macroion at small salt ionic strength. There is a threshold surface charge density for charge inversion. Polymers of multivalent counterions (polyelectrolyte) are effective for charge inversion of a weakly charged rod macroion like DNA with the help of large coions.

PACS numbers: 61.25.Hq, 82.45.-h, 82.20.Wt
Keywords: strongly coupled Coulomb system, electrophoresis, molecular dynamics simulations, charge inversion of DNA by polymer cations

I. INTRODUCTION

The phenomenon of reverting the charge sign of large ions due to other ions and salts in water solution was known to physical chemists as charge inversion or overscreening for half a century [1]. More recently, it also attracted a significant attention of physicists [2–9]. It is now understood that charge inversion is the generic phenomenon that occurs in strongly correlated charged systems. It has far reaching consequences in biological and chemical worlds. In particular, it seems to be a decisive ingredient in modern gene therapy, facilitating the uptake of genes (negative DNA) by predominantly negative cell walls [10].

In our previous papers [6, 7], we worked out a molecular dynamics model adequate to examine charge inversion. More specifically, we studied the electrophoretic mobility problem [7], and showed that a charge inverted complex drifts under the external electric field in the direction determined by its inverted charge. The net charge of the macroion complex was deduced by the force balance, $Q^* \sim \nu\mu$, where μ is the electrophoretic mobility and ν is the solvent friction enhanced by Debye screening of hydrodynamic interactions [11].

The goal of this paper is to extend our studies by addressing three new aspects of charge inversion: dependences on the coion properties, the role of monovalent salt, and the shape of the macroion. Previously we assumed that both counterions and coions are spheres of the same radius. But, anions usually have larger radii than cations for monovalent salt including NaCl. We also assumed that the coions were all monovalent while counterions were multiply charged, which is the necessary condition for charge inversion. Here, we relax these assumptions and examine first the effects of radius and valence of coions on the electrophoretic mobility of a macroion complex immersed in a solution of the $Z^+ : Z^-$ multivalent salt. Moreover, we look at the cases of some experimental environments with monovalent salt that exists as the base of the $Z : 1$ salt, and also the cases of an elongated rod macroion with spherical or polymer counterions (polyelectrolyte).

We take the system of a macroion, coions/counterions and neutral particles, and solve the Newton equations of motion with the Coulombic and Lennard-Jones potential forces under an applied electric field E ($E > 0$). We adopt the repulsive Lennard-Jones potential, $\phi_{LJ} = 4\varepsilon[(\sigma/r_{ij})^{12} - (\sigma/r_{ij})^6]$ for $r_{ij} = |\mathbf{r}_i - \mathbf{r}_j| \le 2^{1/6}\sigma$, and $\phi_{LJ} = -\varepsilon$ otherwise, except for the runs in Fig.7 (Sec.III). Here $\mathbf{r}_i$ is the position vector of the i-th particle, and σ is the sum of the radii of two interacting particles, which are chosen as follows: radius of the macroion R_0, the radii of counterions and coions a^+ and a^-, respectively, with $a^+ = a$ fixed, and neutral particles $a/2$, where a is the unit of length. We relate ε with the temperature by $\varepsilon = k_BT$. The Bjerrum length is thus $\lambda_B = e^2/\epsilon k_BT$ where ϵ is dielectric constant of the solvent. We adopt neutral particles to model the viscous solvent of given temperature and to treat the interactions among the finite-size macroion, counterions, coions and the solvent. Since the hydrodynamic interactions in the electrolyte solvent are screened at short distances comparable to the Debye length [7, 11], the use of thermal bath to drain the Joule heat is not affecting our results. For the details of the employed model and molecular dynamics method, we refer the readers to our previous work [7].

We use the following parameters in this paper unless otherwise specified. The simulation system is a three-dimensional periodic box of the side $L = 32a$. Our

choice of the temperature is $e^2/\epsilon a k_B T = 5$ which implies $a \cong 1.4$Å in water. We set the macroion radius $R_0 = 5a$, charge $Q_0 \sim -80e$, and mass $200m$. The mass of counterions and coions is m, where m is the unit of mass. Each neutral particle has mass $m/2$ and occupies approximately a volume element $(2.1a)^3 \cong (3\text{Å})^3$, except for the volume already occupied by other ions. The external electric field is $E = 0.3\varepsilon/ae$.

In Sec.II we examine the effects of coion radius and valence on charge inversion. Next in Sec.III, we study the effects of monovalent salt. We introduce a rod-shape macroion that can adsorb more counterions than a spherical one for the same surface charge density and find the charge inversion threshold for the rod macroion, which emulates the experiments of DNA charge inversion. Sec.IV will be a brief summary of the present paper.

II. EFFECTS OF DIFFERENT COION RADIUS AND VALENCE

The dependence of electrophoretic mobility on the radius of coions for the fixed counterion radius, $a^+ = a$, is examined. Here, the parameters are: the macroion charge $Q_0 = -80e$, its radius $R_0 = 5a$, the valence of counterions $Z^+ = 3$ (open circles), 5 (filled circles), or 7 (triangles), the valence and number of coions $Z^- = -1$ and $N^- \sim 60$, respectively. The number of counterions is determined from charge neutrality.

In Fig.1, the mobility is reversed (positive) and increases with the ratio of coion to counterion radii up to $a^-/a^+ \approx 1.5$, irrespectively of the counterion valences. This increase is due to geometrical difficulties for two coions condensing on the counterion in avoiding each other if their radius is large, which leads to reduced degree of macroion charge neutralization. This observed increase with the ratio of two ion radii is in line with a previous study of the finite coion size effect for charge inversion [3], and also with condensation of the $Z:1$ electrolyte ions that have size asymmetry [12]. Interestingly, the mobility is extrapolated to the origin when the coion radius is very small in comparison with that of counterions, implying good charge shielding by cloud charges.

The mobility turns into decrease for $a^-/a^+ \geq 1.5$. This trend is also the case for a weak external field $E = 0.1\varepsilon/ae$, thus eliminating the effect of collisions between ions. Instead, this decrease is attributed to the less degree of coion contribution to the charge inversion process. The radial distribution functions tell us that the coions with large radii are more separated from the surface counterions, and that the number of such counterions becomes largest at $a^-/a^+ \approx 1.5$. We showed in our previous paper [6] that "giant" charge inversion is due to the presence of both counterions and coions. Namely, the coions are properly redistributed to minimize the system energy while confining some counterions to the very vicinity of the macroion. With large coions this mechanism does not work, and the number of the counterions near the macroion needs to be reduced.

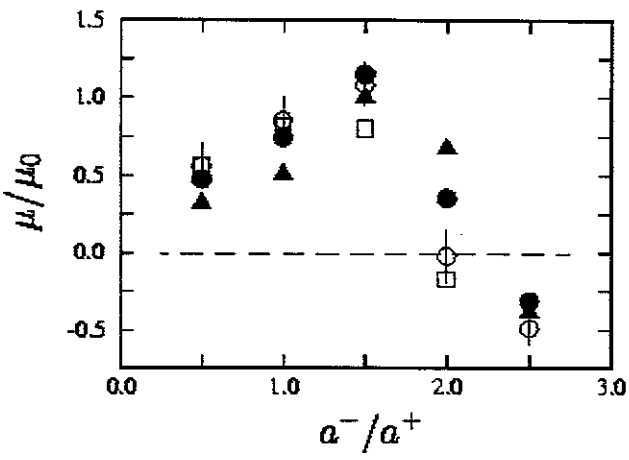

FIG. 1: The dependence of macroion mobility μ on the coion radius is shown as a function of the ratio of the coion to counterion radii a^-/a^+, where $\mu_0 = v_0/(|Q_0|/R_0^2)$ with v_0 being the thermal velocity of neutral particles. Here, the charge and radius of the macroion are $Q_0 \sim -80e$ and $R_0 = 5a$, respectively, the valence of counterions is $Z^+ = 3$ (open circles), 5 (closed circles), 7 (triangles). The external field is $E = 0.3\varepsilon/ae$ for above cases, and $E = 0.1\varepsilon/ae$ for $Z^+ = 3$ (squares). The temperature is $e^2/\epsilon a k_B T = 5$. Coions are monovalent $Z^- = -1$, and their number is approximately $N^- \sim 60$.

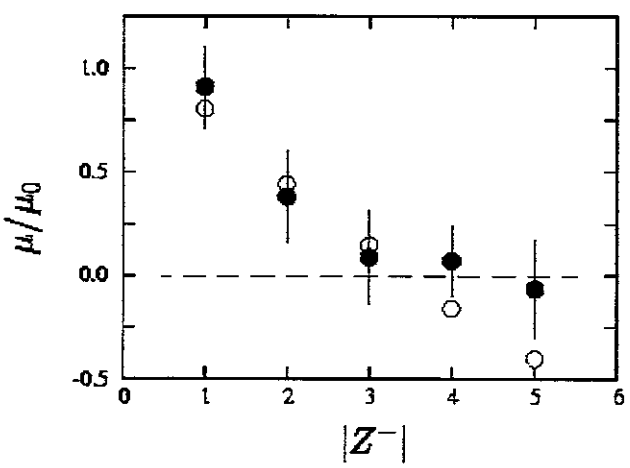

FIG. 2: The effect of the coion valence Z^- on the macroion mobility for fixed counterion valences $Z^+ = 3$ (open circles) and $Z^+ = 4$ (solid circles). The radii of the coions and counterions are equal, $a^-/a^+ = 1$. The external electric field is $E = 0.3\varepsilon/ae$, and the temperature is $e^2/\epsilon a k_B T = 5$.

The effect of coion valence Z^- on electrophoretic mobility for the fixed counterion valences Z^+ is shown in Fig.2. The counterions are either trivalent or tetravalent, the macroion charge and radius are $Q_0 \sim -80e$ and $R_0 = 5a$, respectively. The number of the coions is $N^- = 300/|Z^-|$, and that of the counterions is determined by charge neutrality condition. The coions and counterions have equal radii, $a^- = a^+$. For the monovalent coions, the mobility is reversed and largest. As

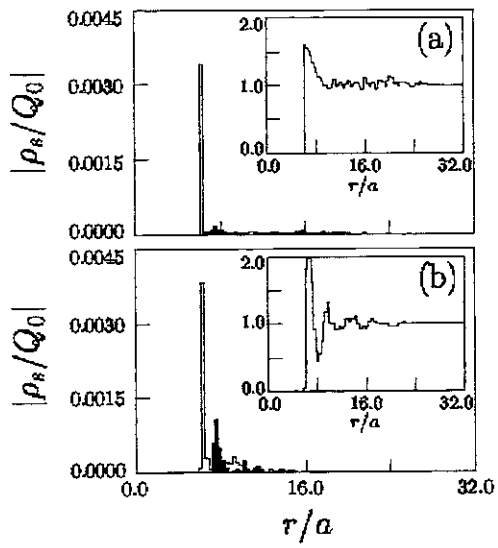

FIG. 3: The radial distribution functions of charge density ρ_s of the counterions (solid) and the coions (shaded) for the coion valence (a) $Z^- = -1$ and (b) $Z^- = -3$ for the runs in Fig.2. The counterion valence is $Z^+ = 3$. The inset panels show the integrated charge distribution $Q(r)/|Q_0|$ for the corresponding charge densities of counterions and coions.

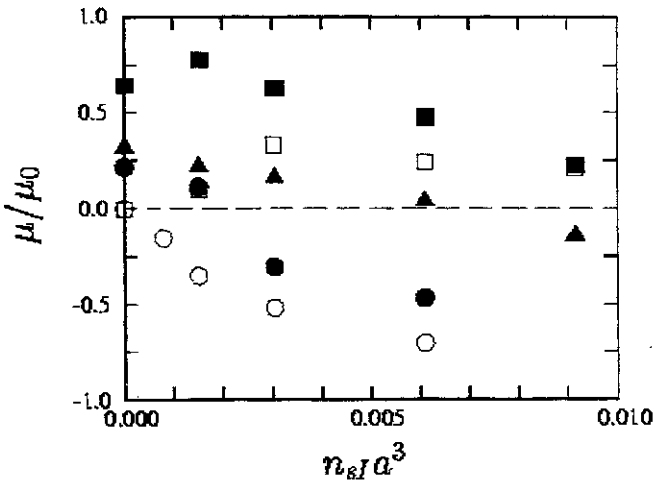

FIG. 4: The mobility of the spherical and rod macroions is shown against the ionic strength of monovalent salt $n_{sI} = 2N^{+1}/L^3$, where N^{+1} is the number of monovalent counterions. Squares and circles are for the spherical macroion, and triangles are for the rod macroion. The parameters for the spherical macroion of radius $R_0 = 5a$ are: $Q_0 = -81e$, $N^{+3} = 37$, $N^- = 30$ (filled squares), $Q_0 = -81e$, $N^{+3} = 27$, $N^- = 0$ (open squares), $Q_0 = -21e$, $N^{+3} = 17$, $N^- = 30$ (filled circles), and $Q_0 = -21e$, $N^{+3} = 7$, $N^- = 0$ (open circles). For the rod macroion, $Q_{rod} = -100e$, $R_{rod} = 5a$, $N^{+3} = 64$, $N^- = 92$ (filled triangles).

the coion valence increases, the magnitude of reversed mobility decreases linearly until the two valences become equal $Z^+ \sim |Z^-|$. The mobility is small but positive for the equal valences, and above that, the mobility turns to negative (non-reversed). These results are consistent with that of Fig.1 in terms of reduced efficiency of charge neutralization by coions.

It is also noted that the result of Fig.2 is in line with the theory of the HNC-MSA integral equations [8] which reported reversed mobility for the case of divalent counterions and coions, $Z^+ = |Z^-| = 2$. The case of $Z^+ = |Z^-|$ is close to the situation of the normal Debye screening, except for the unusually low temperature. We note that, when temperature is low, the Debye theory is not applicable, and one should instead use nonlinear Poisson-Boltzmann theory, which does not provide for charge inversion. On the other hand, when there are strongly charged ions of finite radii and both signs, there occur strong correlations, and even the nonlinear Poisson-Boltzmann theory fails to result in charge inversion.

Indeed, we observe strong correlation of *multivalent* coions with counterions in the radial distribution function of charge density of Fig.3. The panel Fig.3(b) for $|Z^-| = 3$ shows enhanced association of multivalent coions with the surface counterions. The positive macroion complex is surrounded by a sharply formed negatively charged layer, which distinctly separates the macroion complex from the rest of the ion atmosphere. The integrated charge distribution $Q(r) = \int \sum_s \rho_s(r')d^3r'$ in the inset panel of Fig.3(b) better illustrates this situation, where the integration starts at the macroion surface $r = R_0$ and the summation goes over counterions and coions. The width of the positively charged layer becomes as small as $1.3a$ for $Z^- = -3$, whereas it is $3.4a$ for $Z^- = -1$ in Fig.3(a). Each multivalent coion is thus firmly condensing to the counterions and efficiently reducing the positive charges of the macroion complex.

III. EFFECTS OF MONOVALENT SALT AND ROD-SHAPED MACROION

Now we study the effects of monovalent salt that exists as the base component to the multivalent salt. We treat the cases of both a spherical macroion and a rod-shape macroion placed in the solution of Z:1 and 1:1 salt of spherical ions. The common parameters in this section are the valence of multivalent counterions $Z = 3$, the equal radii of coions and counterions $a^- = a^+ = a$.

Figure 4 shows the dependence of mobility against the ionic strength of monovalent salt, $n_{sI} = 2N^{+1}/L^3$, where N^{+1} is the number of monovalent counterions which is equal to the number of matching monovalent coions. The salt ionic strength for $N^{+1} = 50$ is $n_{sI} \sim 0.0031a^{-3}$. Here, the common normalization $\mu_0 = v_0/E_0$ with $E_0 = |Q_0^{(0)}|/(R_0^{(0)})^2$ is used for the macroions of the spherical and rod shapes, where $Q_0^{(0)} = -81e$ and $R_0^{(0)} = 5a$.

Interestingly, for a strongly charged macroion of the spherical shape with charge $Q_0 = -81e$ whose surface charge density is $\sigma_{sp} = Q_0/4\pi R_0^2 \sim 0.25e/a^2$ (filled squares), addition of small amount of monovalent salt en-

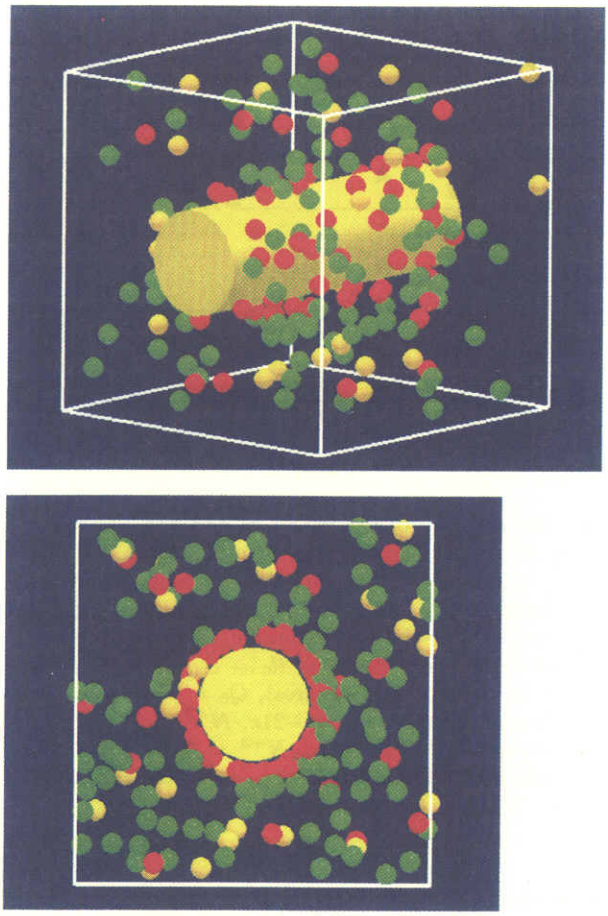

FIG. 5: The bird's-eye view (top) and the side view (bottom) of all the ions for the rod macroion that corresponds to $Q_{rod} = -100e$ and $n_{sI}a^3 \sim 0.0015$ data point in Fig.4. The small ions are trivalent counterions $N^{+3} = 64$ (red), monovalent coions $N^- = 92$ (green), and the monovalent positive salt $N^+ = 25$ (yellow). (Neutral particles are not shown).

hances the reversed mobility. Even for the case without excess Z-ions for which $N^{+3} = |Q_0|/eZ$ (open squares), charge inversion is induced by monovalent salt. This is due to cooperation of monovalent and multivalent counterions. Namely, the monovalent counterions fill the spaces among the Z-ions on the macroion surface, thus adding to the inverted charge of the macroion complex. The Wigner-Seitz cell radius is $R_W = 2R_0(eZ/|Q_0|)^{1/2} \sim 1.9a$. This enhancement occurs for the ionic strength of monovalent salt less than that of the free Z-ions, $n_{sI} < \frac{1}{2}n_{ZI}$. The Debye length corresponding to this inequality is $\lambda_D = (\epsilon k_B T/8\pi n_{sI}e^2)^{1/2} > 2a \approx R_W$. More amount of monovalent salt decreases the reversed mobility, which is extrapolated to null at $n_{sI} \sim 0.013a^{-3}$ or $N^{+1} \sim 200$.

The open and filled circles in Fig. 4 are the cases of a weakly charged macroion of the spherical shape with charge $Q_0 = -21e$ for the number of trivalent Z-ions $N^{+3} = 7$ and 17, respectively. The surface charge density

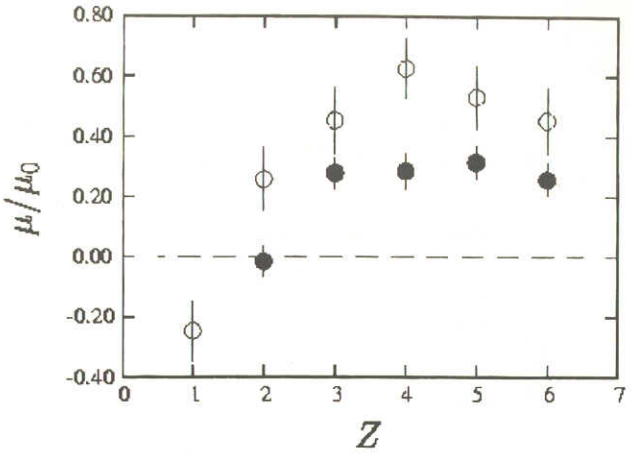

FIG. 6: Dependence of the mobility on the valence of the counterions Z for a macroion of the rod shape with radius $R_{rod} = 5a$ and charge $Q_{rod} = -100e$ (filled circles). The number of monovalent coions is $N^- \sim 60$. The spherical macroion case with $R_0 = 5a$ and $Q_0 = -80e$ is shown by open circles.

is $\sigma_{sp} = 0.067e/a^2$. For the former, the number of the Z-ions is just sufficient to neutralize the macroion; charge inversion is not observed. For the latter case, there are ten extra Z-ions besides the $|Q_0|/eZ = 7$ neutralizing ions. The mobility is reversed at zero salt, and decreases monotonically with the salt ionic strength, which turns to normal (non-reversed) when the ionic strength of extra Z-ions is dominated by that of the monovalent salt.

We have interpreted that the above rapid decrease in the mobility with salt ionic strength for the weakly charged macroion arises from the spherical effects. Namely, a small number of adsorbed Z-ions on the macroion is not sufficient to maintain correlations by overcoming thermal fluctuations. Thus, we proceed to adopt a macroion of the rod shape, extending in full length to the z direction, with the radius $R_{rod} = 5a$. The surface charge density for $Q_{rod} = -100e$ is $\sigma_{rod} = Q_{rod}/2\pi R_{rod}L \sim 0.10e/a^2$ (filled triangles). For the rod macroion, the reversed mobility is three times more persistent to monovalent salt than for the spherical macroion with similar surface charge density.

The large reversed mobility observed in Fig.4 is associated with the Z-ion network formation on the surface of the macroion, irrespectively of spherical or rod shapes. Fig.5 shows the case of the rod macroion. As with the case of the strongly charged spherical macroion (cf. Fig.1 of [7]), majority (70%) of the Z-ions are adsorbed on the macroion surface, which is more than enough for charge neutrality requirement. By contrast, most of the monovalent counterions (80%) are detached from the macroion and homogeneously distributed. This is due to stronger binding forces of the multivalent counterions to the macroion than for monovalent ones. The coions are condensing to the topside of the counterions on

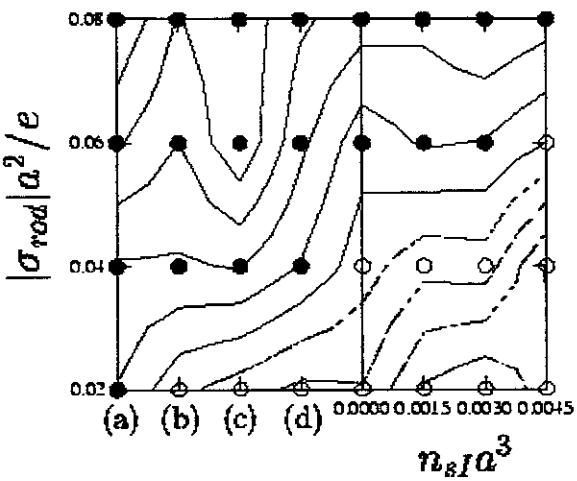

FIG. 7: (Right:) The electrophoretic mobility μ of a rod macroion of radius $R_{rod} = 5a$ and spherical ions with $a^-/a^+ = 1.0$, in the (n_{sI}, σ_{rod}) domain, where $\sigma_{rod} = Q_{rod}/2\pi R_{rod}L$ is the surface charge density of the macroion. (Left:) (a) polymer Z-ions with $a^-/a^+ = 1.5$, and the Lennard-Jones attraction force, (b) polymer Z-ions with $a^-/a^+ = 1.5$, (c) polymer Z-ions with $a^-/a^+ = 1.0$, (d) all separate ions with $a^-/a^+ = 1.5$, at zero monovalent salt. The solid (dashed) contours correspond to reversed (non-reversed) mobility in the $0.0055\mu_0$ interval, with the first solid contour being $\mu = 0$. The data points with filled and open circles show inverted and non-inverted mobilities, respectively.

the macroion surface, and charge neutralization occurs in about $3a$ from the surface.

Since we have learned above that the geometry (shape) of the macroion affects charge inversion, we are tempted to reexamine the effect of counterion valence on the electrophoretic mobility. Figure 6 shows the mobility against the valence Z. The surface charge densities are $\sigma_{sp} = 0.26e/a^2$ for the sphere and $\sigma_{rod} = 0.10e/a^2$ for the rod. We showed previously that the mobility for the spherical macroion peaks around $Z \approx 4$ (open circles) [7]. The Wigner-Seitz cell radius for $Z = 4$ is $R_W \sim 2.2a$ which is comparable to the radius of the macroion $R_0 = 5a$. The mobility for the rod macroion becomes reversed for $Z > 2$ and then levels off, in contrast to the spherical macroion of the same radius. Thus, the rod geometry even with a finite radius $R_{rod} \sim 2R_W$ is already close to the plane geometry.

The mobility of a rod macroion against surface charge density σ_{rod} and ionic strength of monovalent salt n_{sI} for the $a^-/a^+ = 1$ case is shown by contours in the right portion of Fig.7 (to the right of the dividing line), where solid (dashed) contour corresponds to positive (negative) mobility. The common parameters are: trivalent counterions, the number of coions $N^- \sim 60$, the temperature $e^2/\epsilon a k_B T = 5$, and the external field $E = 0.1\varepsilon/ae$. We use in this section the normalization of the mobility $\mu_0 = v_0 R_{rod}L/2|Q_{rod}|$, which is based on the rod surface electric field. If all the counterions are adsorbed to the rod, their surface charge density will be $\sigma^+ \sim |\sigma_{rod}| + 0.06e/a^2$. The reversed mobility is reduced or becomes more negative by addition of monovalent salt. Charge inversion of a *smooth* rod requires the minimum surface charge density $0.05e/a^2$ for $n_{sI} = 0$ and $a^-/a^+ = 1$ with the electrostatic forces only. This value is 2.5 times above the average surface charge density of the DNA double helix $\sigma_{DNA} \approx 0.02e/a^2$, as $a \cong 1.4$Å.

In reality, anions frequently have larger radii than cations, and cations are generally positive polyelectrolyte for gene delivery [10]. Also, the chemical groups of DNA may exert short-range attractive forces on surface ions through hydrogen bonds or hydrophobicity. The data points aligned vertically to the left of the dividing line show the mobility for different cases: (a) polymer Z-ions with large coions $a^-/a^+ = 1.5$ and the Lennard-Jones attraction force, (b) polymer Z-ions with $a^-/a^+ = 1.5$, (c) polymer Z-ions with $a^-/a^+ = 1.0$, (d) spherical ions with $a^-/a^+ = 1.5$, all at zero monovalent salt. Here, the "polymer" stands for the use of the spring-beads model where three Z-ions in a row are connected by a chain of the finite length approximately $2.3a$. Other parameters and conditions are the same as before. The threshold surface charge density becomes small as we migrate from (d) to (c), and then to (b). The threshold decreases to $0.035e/a^2$ for the large coions with $a^-/a^+ = 1.5$, and to $0.025e/a^2$ for polymer Z-ions with $a^-/a^+ = 1.5$, at zero monovalent salt.

Figure 7(a) shows the case where, on top of the setting of (b), the short-range attraction force is included in the Lennard-Jones potential by extending its range to $r > 2^{1/6}\sigma$. The depth of the attraction potential is $\varepsilon = k_B T$. Then, the threshold of charge inversion drops to below the average surface charge density of DNA. The mobility for $\sigma_{rod} = 0.02e/a^2$ at zero monovalent salt is $\mu \approx 0.005\mu_0$.

The reversed mobility can be obtained without inclusion of the Lennard-Jones attractive potential if the chain length of the polymer counterions is longer than some value. For example, with the chain length five for the valence $Z = 3$ and the large coion radius $a^-/a^+ = 1.5$, we get $\mu \approx 0.006\mu_0$. The radial distribution function shows adsorption of the counterions on the macroion surface. The peak of the integrated charges of the macroion complex occurs in the very vicinity of the macroion surface, which amounts to $Q_{peak} \approx 1.7|Q_{rod}|$ for the chain length five.

These results mentioned above are consistent with a theory that predicts charge inversion for the polymer cations of unit charges and discrete surface charges [13]. On the other hand, molecular dynamics results require more strict conditions for charge inversion of DNA. This discrepancy might be attributed to that the theory is based on a static thermodynamics model that does not treat discrete ions and thermal fluctuations observed in the molecular dynamics simulations.

IV. SUMMARY

We showed three things in this paper. First, a large coion radius (up to $a^-/a^+ \approx 1.5$) plays a positive role for charge inversion while a large coion valence does a negative role, for fixed radius and valence of counterions. The reversed mobility started from nearly null at very small coion radius; it increased with the ratio of the coion to counterion radii a^-/a^+, and peaked at the ratio $a^-/a^+ \approx 1.5$. It decreased for further increase in the ratio due to the loss of coion correlations, since coions need to be involved for large charge inversion. The reversed mobility decreased with the ratio of the coion to counterion valences Z^-/Z^+, and the charge inversion was terminated for the coion valence exceeding that of the counterions.

Second, monovalent salt of large ionic strength suppressed reversed mobility that was induced by the Z:1 salt, except that small amount of the monovalent salt enhanced reversed mobility for a strongly charged macroion. For a weakly charged macroion, this enhancement region was apparently small and not detected.

Thirdly, there was a threshold of surface charge density for charge inversion due to thermal agitations of surface counterions. A rod-shaped macroion was more persistent to monovalent salt than a spherical macroion. The threshold for the rod macroion was around $\sigma_{rod} \sim 0.05e/a^2$ at $e^2/\epsilon a k_B T = 5$. This threshold was lowered down to below the (average) surface charge density of DNA when short polymers of multivalent counterions were used with the help of large coions.

Acknowledgments

The computations of the present study were performed with the use of Origin 3800s of the University of Minnesota Supercomputing Institute, and the vpp800/13 supercomputer system of the Institute for Space and Astronautical Science (Japan).

[1] H.G. Bungenberg de Jong, *Colloid Science, vol.2*, edited by H.R. Kruyt (Elsevier, 1949) 259-330.

[2] E.Gonzales-Tovar, M.Lozada-Cassou, and D.J. Henderson, *J. Chem.Phys. 83*, 361 (1985).

[3] H.Greberg, and R.Kjellander, *J.Chem.Phys. 108*, 2940 (1998).

[4] T.T.Nguyen, A.Yu. Grosberg and B.I. Shklovskii, *Phys. Rev. Lett. 85*, 1568 (2000).

[5] R.Messina, C.Holm and K.Kremer, *Phys.Rev.Lett. 85*, 872 (2000).

[6] M.Tanaka and A.Yu. Grosberg, *J.Chem.Phys. 115*, 567 (2001).

[7] M.Tanaka and A.Yu. Grosberg, *Euro.Phys.J., E7*, 371 (2002).

[8] M.Lozada-Cassou, E.Gonzales-Tovar, and W.Olivares, *Phys.Rev. E 60*, R17 (1999); M.Lozada-Cassou and E.Gonzales-Tovar, *J.Colloid Interf.Sci. 239*, 285 (2001).

[9] A.Yu. Grosberg. T.T. Nguyen, and B.I. Shklovskii, *Reviews Modern Phys., 74*, 329 (2002).

[10] A.V.Kabanov, V.A.Kavanov, *Bioconj.Chem., 6*, 7 (1995).

[11] D.Long, J.-L.Viovy, and A.Ajdari, *Phys.Rev.Lett., 76*, 3858 (1996).

[12] A.Z.Panagiotopoulos and M.E.Fisher, *Phys.Rev.Lett. 88*, 045701 (2002).

[13] T.T.Nguyen and B.I. Shklovskii, *Phys.Rev.Lett.*, 018101 (2002).